Paper No. 20

ON THE VALIDITY OF LIFTING LINE CONCEPTS IN ROTOR ANALYSIS.

Th. van Holten
Delft University of Technology
Dept. of Aeronautical Engineering
Delft, Netherlands.

Summary

Using the acceleration potential description of flow fields combined with a matched asymptotic expansion technique, a higher-order lifting line theory can be developed which takes into account all the unsteady, yawed flow effects encountered by helicopter blades. This theory points out several errors in the usual lifting line methods of rotor analysis.

1. Introduction

There is a trend nowadays to use lifting surface methods in the theoretical analysis of aerodynamic loads on rotorblades (e.g. ref. 1). It is easy to see why attempts are made to improve upon the lifting line analyses that have been used for so long:

a) The basic concepts of lifting line theory were evolved by Prandtl, in relation with his classical work on straight, high aspect ratio wings in steady motion. His fundamental ideas were: the wingsection characteristics may be treated by two-dimensional theory, whilst the three-dimensional character of the flow is taken into account by the calculation of an "effective" angle of attack. The latter differs from the geometrical angle of attack by the effect of the downwash induced by the wake of a lifting vortex line. Prandtl's method was never intended to be applied to cases of unsteady and/or yawed flow such as encountered in rotor aerodynamics. And indeed, straightforward, intuitive application of Prandtl's ideas to the analysis of a helicopter rotor in forward flight leads to severe problems. In the past these problems have been solved by ingenious "tricks", effective enough, but sometimes rather hard to justify.

For example, one was forced to introduce the simple cos-Λ sweep correction in order to rescue the concept of two-dimensional section characteristics in the yawed flow environment. The simple sweep correction originates from the well known discussion of a wind tunnel through which an infinite wing is sliding, and is valuable as a qualitative explanation of sweep effects. Nevertheless, it is certainly not suitable for the quantitative analysis of a wing with rapidly varying load in spanwise direction.

As a further example may serve the observation that in fixed wing analysis one has rejected altogether the use of lifting line theory in unsteady flow: the shed vorticity (fig. 1) of a vortex line would cause infinite values of the induced downwash. The latter means in fact, that one should take into account the distribution of shed vorticity over the chord, and any line-concept is thus lost in the process.

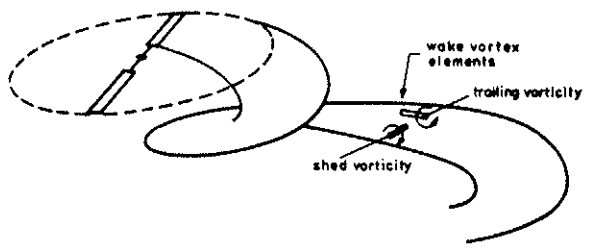

Fig.1: Wake vorticity of a helicopterblade.

Similar problems have prevented the use of an effective angle of attack concept in the case of swept wings. One of the usual procedures for avoiding such problems in rotoranalysis has been to replace the continuous wake by a system of discrete vortex elements, but then uncertainties arise as to what is the best distribution of the vortex elements, both time- and spanwise relative to the points where the induced downwash is calculated.

b) As mentioned already, the chordwise pressure distribution is in lifting line theory assumed to correspond to the distribution over a two-dimensional aerofoil. Since this approximation is not justified in many practical cases, not even in the

case of high aspect ratio rotorblades (where the rapid spanwise load variations cause low aspect ratio effects) it is impossible to calculate pitching moments by line theory, let alone to predict compressibility effects from calculated isobar contours, etc.

These are, very briefly, the reasons why more sophisticated methods are desired for certain applications. Unfortunately, lifting surface methods are by no means superior to lifting line methods in all respects. An obvious point in favour of lifting line theory is the amount of computing time needed. Another important point to consider is, that many phenomena of rotor aerodynamics, e.g. dynamic stalling and dynamic compressibility effects, cannot yet be investigated and quantitatively predicted in any other way than by experimental methods. As soon as such experiments take the form of two-dimensional wind tunnel tests, one is making use of typical lifting line concepts such as section characteristics and effective angles of attack. The incorporation of experimental results into lifting line analysis is thus a very natural process. On the other hand, a similar blending of theory and experiment is more difficult to achieve when lifting surface methods are used.

There is a third analytical approach in existence which combines the advantages of both lifting line and lifting surface theory. This approach is the higher-order lifting line theory, derived by a "matched asymptotic expansion" technique (refs. 2 and 3). Using the acceleration potential for the description of the flow field, it is easy to develop classical lifting line theory systematically and rigorously, so that one can correctly take into account the effects of non-steady and/or yawed flow. A higher-order approximation is also relatively easily derived, leading to an improved surface pressure distribution. The correction of the pressure distribution due to higher order effects is additive to the two-dimensional pressure distribution of the first order theory, so that the basic concept of two-dimensional section characteristics is not lost. Finally, although continuous wake representations are used in the theory, the method is efficient in numerical applications. An outline of rotor calculations using the asymptotic method will be given in the chapters 2, 3 and 4 of the present paper. The paper then proceeds, to concentrate on the conclusions concerning the validity of conventional lifting line methods and related concepts, drawn from the above mentioned references and from continued investigations. The aim is, to provide a better understanding of lifting line theory, to point out where conventional methods have gone wrong in unsteady, yawed flow analysis, and to show how these methods should be modified to solve the problems. It is also pointed out under what circumstances the basic assumption of approximate two-dimensionality will certainly break down, and how the theory may then be remedied.

2. Brief review of the theory of the acceleration potential

The acceleration potential was first introduced in 1936 by Prandtl for the analysis of lifting surfaces in incompressible flow. The quantity $-p/\rho$ was called the acceleration potential of the flow, since according to Euler's equation

$$\frac{D\underline{V}}{Dt} = \frac{\partial \underline{V}}{\partial t} + (\underline{V}.\underline{\nabla})\underline{V} = \text{grad}\ (-\frac{p}{\rho}) \tag{1}$$

the gradient of $-p/\rho$ equals the acceleration of the fluid particles. Writing $\underline{V} = \underline{U} + \underline{V}'$ and $p = p_\infty + p'$ where $\underline{U}$ is the undisturbed velocity (taken to be independent of the space- and time coordinates) and $\underline{V}'$ is the perturbation velocity, linearization of Euler's equation leads to

$$\frac{D\underline{V}}{Dt} = \frac{\partial \underline{V}'}{\partial t} + (\underline{U}.\underline{\nabla})\underline{V}' = -\frac{1}{\rho}\ \text{grad}\ p' \tag{2}$$

which yields, on taking the divergence of all the terms of (2) and applying the continuity equation div $\underline{V}' = 0$, the Laplace equation for p':

$$\text{div grad } p' = \frac{\partial^2 p'}{\partial x^2} + \frac{\partial^2 p'}{\partial y^2} + \frac{\partial^2 p'}{\partial z^2} = 0 \qquad (3)$$

In the following the primes will be omitted for convenience, so that p and $\underline{V}$ will both denote perturbation quantities.
Eq. (2) expresses the fact that in the linearized theory considered here, the velocity in a point of the field is found by integrating the acceleration of a particle of air coming from far upstream, whilst during this integration the particle's trajectory may be approximated by its straight, unperturbed trajectory.
Boundary conditions must accordingly be applied to flat surfaces, parallel to the undisturbed flow.
In incompressible flow fields the pressure perturbation p cannot display any discontinuities except on the solid boundaries of the field. This is the main advantage of the pressure formulation: describing the field in terms of the pressure, no such things like free vortex sheets can enter into the mathematical formulation of the problem.

3. Boundary value problem of the helicopterblade

The notations used in the rotoranalysis are shown in fig. 2. The tip path plane includes the angle α_r with the free stream velocity $\underline{U}$. The blade includes a coning angle a_o with the tip path plane, and it executes a periodic pitching motion when moving around the azimuth, the latter denoted by the angle ψ_b. Expressed in terms of the blade-fixed coordinates x_b, y_b, z_b, shown in fig. 2, the boundary value problem now becomes as follows. The field of pressure perturbations around a blade must satisfy Laplace's equation:

$$\frac{\partial^2 p}{\partial x_b^2} + \frac{\partial^2 p}{\partial y_b^2} + \frac{\partial^2 p}{\partial z_b^2} = 0 \qquad (4)$$

The pressure perturbations must vanish at large distances from the blade:

$$p \to 0 \quad \text{for } x_b^2 + y_b^2 + z_b^2 \to \infty \qquad (5)$$

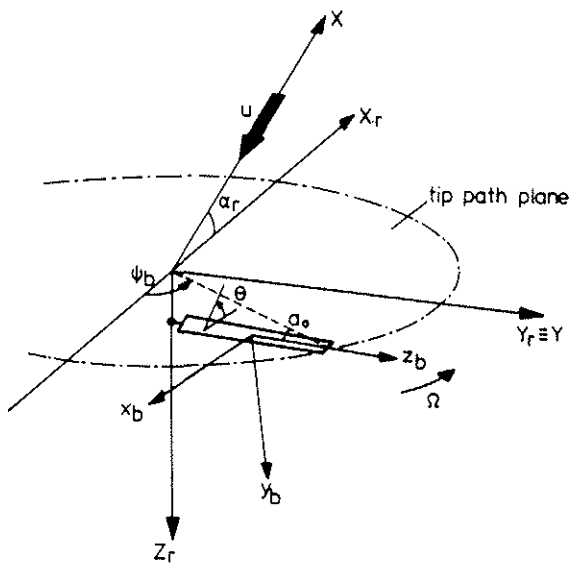

Fig. 2: Notations rotor analysis

The component of the pressure gradient normal to the blade surface must according to eq. (2) assume a certain value, specified as a function of azimuth angle ψ_b, spanwise location z_b, and chordwise position x_b:

$$-\frac{1}{\rho\Omega^2 R}\frac{\partial p}{\partial y_b} = F_1(\psi_b, z_b) + \frac{x_b}{R} F_2(\psi_b, z_b) \text{ on the blade} \qquad (6)$$

The functions F_1 and F_2, containing as parameters the blade geometry and rotor working conditions, are given explicitly in ref. 2. Along the leading edge of the blade there is a streamline kink, which implies that there is pressure singularity:

$$p \to -\infty \text{ along the leading edge} \qquad (7)$$

The magnitude of the singularity should be such that the flow becomes tangential to the blade surface. Since we have already required by eq. (6) that the curvature

of the flow on the blade surface is correct, it is sufficient to require the flow to be tangential at one line of the blade only. A convenient choice is the mid-chord line, where the velocity component w normal to the blade surface is specified:

$$\frac{w}{\Omega R} = F_3\ (\psi_b, z_b) \text{ along the mid-chord line} \tag{8}$$

4. Asymptotic solution

In order to find an approximate solution of the boundary value problem we introduce the following physical assumption: the variations of the pressure in spanwise direction have a characteristic length of the order of the span, whereas the variations of the pressure in chordwise direction have a characteristic length of the order of the chord.

Evidently, this assumption can be valid only in the socalled near field of the blade, i.e. the field close to the blade surface. Rewritten in terms of the characteristic coordinates x_b/c, y_b/c and z_b/R (c and R denote chord and span respectively), Laplace's equation reads:

$$\frac{\partial^2 p}{\partial (x_b/c)^2} + \frac{\partial^2 p}{\partial (y_b/c)^2} = -\frac{1}{A^2}\frac{\partial^2 p}{\partial (z_b/R)^2} \tag{9}$$

where A is the aspect ratio R/c. On the grounds of the physical assumption mentioned above, the partial derivatives in (9) are all of the same order of magnitude. It follows immediately from (9) that p satisfies a two-dimensional Laplace equation when A is very large ($A \to \infty$). One may go one step further, and write the near pressure field in the following form:

$$p = p_{\text{two-dim}} + \frac{1}{A} p_1 + \frac{1}{A^2} p_2 + \ldots \qquad \text{for } A \to \infty \tag{10}$$

This is an asymptotic expression, in which the first term is the two-dimensional pressure field, whereas the other terms describe the way in which the pressure field becomes two-dimensional when the aspect ratio grows larger and larger. Substituting (10) into (9) and equating terms of equal order, one arrives at the following conclusion: even when terms of order $O(A^{-1})$ are included, the pressure field still satisfies a two-dimensional Laplace equation:

$$\frac{\partial^2 p}{\partial x_b^2} + \frac{\partial^2 p}{\partial y_b^2} = 0 \text{ up to order } O(A^{-1}) \tag{11}$$

In the next, higher-order, approximation p satisfies a two-dimensional Poisson-equation:

$$\frac{\partial^2 p}{\partial x_b^2} + \frac{\partial^2 p}{\partial y_b^2} = -\frac{\partial^2}{\partial z_b^2}\left(p_{\text{two-dim}}\right) \text{ up to order } O(A^{-2}) \tag{12}$$

where $p_{\text{two-dim}}$ is the solution obtained from (11).

Once again, eqs. (11) and (12) are valid only in the near field. It is possible to obtain a solution for the complete pressure field by a socalled matching procedure (see ref. 2). The structure of the final solution thus found for the first order problem (up to order A^{-1}) is shown in the following expression, and will be explained briefly:

$$\frac{p}{\rho\Omega^2 R^2} = \underbrace{\frac{c_{t_1}(\psi_b, z_b)}{\pi}\frac{\sin\varphi}{\cosh\eta+\cos\varphi} + \frac{F_1(\psi_b, z_b)}{2A} e^{-\eta}\sin\varphi +}_{\text{NEAR PRESSURE FIELD}}$$

$$+ \underbrace{\frac{p_{dip}}{\rho\Omega^2 R^2}(r, \chi, z_b, \psi_b)}_{\text{FAR PRESSURE FIELD}} +$$

$$\underbrace{- \{c_{t_1}(\psi_b, z_b) + \frac{\pi}{4A} F_1(\psi_b, z_b)\} \, c \, \frac{\sin\chi}{2\pi r}}_{\text{CORRECTION TERM (COMMON PART)}} \qquad (13)$$

Near field. The symbols η and φ denote elliptic coordinates, explained in fig. 3 and conforming to the transformation formulae: $x_b = c/2 . \cosh\eta . \cos\varphi$

$y_b = c/2 . \sinh\eta . \sin\varphi$.

It may be shown that the near field terms in eq. (13) satisfy the two-dimensional Laplace equation and also satisfy the boundary conditions (6) and (7). The near field depends parametrically upon the azimuth-angle ψ_b and spanwise coordinate z_b, via the functions $c_{t_1}(\psi_b, z_b)$ and $F_1(\psi_b, z_b)$. F_1 is the same function as occurs in boundary condition (6), and the local thrust coefficient c_{t_1} is defined as $c_{t_1} = \frac{\ell_1}{\rho\Omega^2 R^2 c}$ (the lift ℓ_1 is taken positive in negative y_b-direction). The index 1 in the lift ℓ_1 is used, since another contribution to the lift follows from the second near field term with F_1.

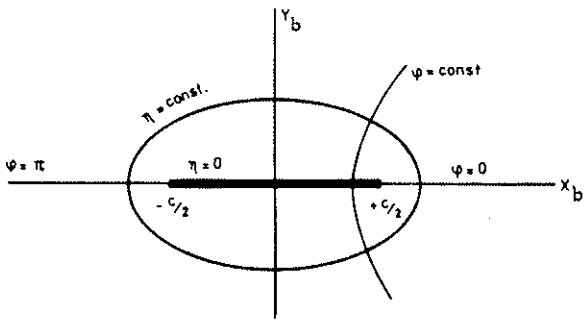

Fig.3: Elliptical coordinate system

The first term, depending on c_{t_1}, is the pressure field of a flat plate aerofoil, becoming singular along the leading edge ($\eta = 0$, $\varphi = \pi$) and having $\partial p/\partial y_b = 0$ on the blade. It is the pressure field causing the streamlines to be kinked at the leading edge so that immediately past the leading edge the tangential flow condition is satisfied. Any further streamline curvature required by the periodic pitching motion of the blade is taken care of by the second pressure field depending on F_1.

Far field. It may be shown that at large distances from the blade the pressure field simplifies to the field of a line of pressure dipoles $p_{dip}(r, \chi, z_b, \psi_b)$, a socalled lifting line. The coordinates r, χ, z_b are cylindrical coordinates centered around the mid-chord line of the blade. The strength of the pressure dipoles along the lifting line is equal to the lift on the blade.

Correction term or the socalled "common part". In order to construct an expression for the blade's pressure field that is valid throughout the field, at large distances as well as close to the blade, the near- and far field have been summed, and a correction term is subtracted. This correction term has been chosen such, that far from the blade it cancels the near field to the required order of accuracy, so that only the far field remains. Close to the blade surface, the correction term cancels the far field, so that only the near field remains there. The correction term has the form of a two-dimensional pressure dipole, with dipole strength equal to the total lift of the section whose position is given by ψ_b, z_b.

Having obtained now an expression for the pressure field around the blade of a helicopter rotor, we can calculate the velocity perturbation in y_b-direction along the mid-chord line by using the equation of motion (2). The evaluation of the velocity is equivalent to the computation of the velocity acquired by a particle of air travelling through the known pressure field and passing the considered collocation point on the mid-chord line at the required time t_o. In the linearized

theory the trajectory of the particle is approximated by a straight line (in the XYZ-system of fig. 2) parallel to the unperturbed flow velocity $\underline{U}$. The position of the particle relative to the rotating blades is thus known at any instant of time, as well as the pressure gradient component $\partial p/\partial y_b$ "experienced" by the particle, and the final velocity perturbation is found by solving the integral:

$$\frac{w}{\Omega R} = -\frac{1}{\rho \Omega R} \int_{-\infty}^{t_o} \frac{\partial p}{\partial y_b}(t)\, dt \text{ summed over all the blades} \qquad (14)$$

where $-\frac{1}{\rho}\frac{\partial p}{\partial y_b}(t)$ is the vertical acceleration experienced by the particle, when it moves through the pressure field of the rotor.

It is shown in ref. 2 that all the terms in (13) can be expressed in closed form, so that the velocity calculation amounts to one-dimensional integration with respect to time, replacing the two-dimensional integration over the skewed helical vortex sheets needed in the vortex theory.
Equating $\frac{w}{\Omega R}$ according to (14) to $\frac{w}{\Omega R}$ as required by the boundary condition (8) results in the final integral equation for the unknown function $c_{t_1}(\psi_b, z_b)$.

It can be shown (chapter 5) that the method described above reduces to Prandtl's classical lifting line theory in the case of a straight wing in steady parallel flow. However, when the present theory is applied to the case of the helicopter blade with its unsteady, yawed flow, certain essential departures from the conventional lifting line methods are bound to occur. This may be concluded from the fact that - in contrast to conventional methods - no difficulties at all are met with respect to singular values of the downwash. Neither is anything like a special sweep correction needed in order to make the method work. It is apparently worthwhile to investigate the differences between Prandtl's lifting line theory and the asymptotic theory outlined above, in order to obtain a better understanding of lifting line theory, and to see where conventional rotor analyses have gone wrong.

5. Lifting line theory in unsteady flow

Instead of the more complicated case of a rotorblade, an easy "model" case will be considered, i.e. the rectangular, uncambered wing (notations: fig. 4). As a preliminary we will write down the expressions for the unswept wing ($\Lambda = 0$) in steady flow, in which case the pressure field of the wing is given by (compare eq. (13)):

$$\frac{p}{\frac{1}{2}\rho U^2} = -\frac{c_\ell(z)}{\pi}\frac{\sin\varphi}{\cosh\eta+\cos\varphi} +$$

$$+ \frac{p_{dip}}{\frac{1}{2}\rho U^2}(r,\chi,z) + c_\ell(z)\; c\,\frac{\sin\chi}{2\pi r}$$

$$\text{to order } 0(A^{-1}) \qquad (15)$$

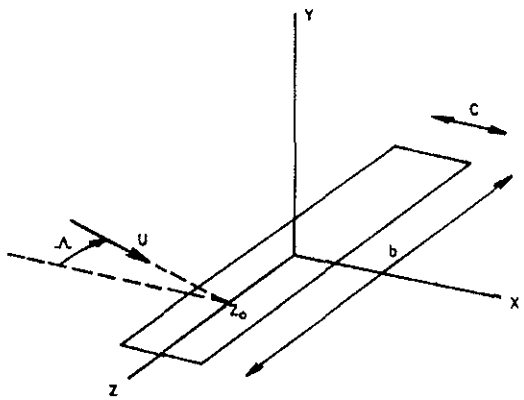

Fig. 4: Notations straight, rectangular wing.

The vertical velocity perturbation along the mid-chord line is calculated using the equation of motion (2) in a manner analogous to eq. (14). Now the first term in the r.h.s. of (15) is the pressure field of a two-dimensional flat plate aerofoil. Consequently, this term contributes a velocity $\left(\frac{v}{U}\right)_{\text{near field}} = -\frac{c_\ell(z)}{2\pi}$, as in two-dimensional aerofoil theory.

Integration of the other two terms in the r.h.s. of (15) yields:

$$\left(\frac{v}{U}\right)_{\substack{\text{far field+}\\ \text{common part}}} = \frac{1}{8\pi} \int_{-b/2}^{+b/2} \frac{d(c_\ell . c)/dz}{\zeta - z}\, d\zeta \qquad (16)$$

which evidently equals, what is usually called the "induced angle of attack" v_i/U (with a minus-sign), in vortex theory considered to be caused by the trailing vorticity of the lifting vortex line. In the pressure theory it is caused by the lifting pressure dipole line, together with the common part term consisting of a two-dimensional pressure dipole.

If $\alpha_o(z)$ is the incidence of the wingchords, we obtain as the integral equation for the function $c_\ell(z)$:

$$-\alpha_o(z) = \left(\frac{v}{U}\right)_{\text{near field}} + \left(\frac{v}{U}\right)_{\substack{\text{far field+}\\ \text{common part}}} = -\frac{c_\ell(z)}{2\pi} - \frac{v_i}{U}(z)$$

or, rewritten:

$$c_\ell(z) = 2\pi \{\alpha_o(z) - v_i/U(z)\} \qquad (17)$$

which is Prandtl's classical integral equation, stating that a wingsection behaves like a two-dimensional aerofoil placed at an effective angle of attack $\alpha_o - v_i/U$. It does not appear at first sight that we have found anything new, except perhaps the error estimate that Prandtl's theory neglects effects of order $O(A^{-2})$. In fact, however, eq. (17) does on closer consideration reveal a shortcoming in Prandtl's classical model. For, in the asymptotic approach to lifting line theory v_i was found as the contributions of the pressure dipole line together with the common part term. Translated into vortex terminology, this means that v_i is the velocity due to the lifting vortex and its associated trailing vorticity together with the velocity due to a two-dimensional vortex of equal local strength but with opposite direction (see fig. 5). Naturally, this does not affect the quantitative results in steady flow: the contribution of the two-dimensional vortex to v_i is zero.

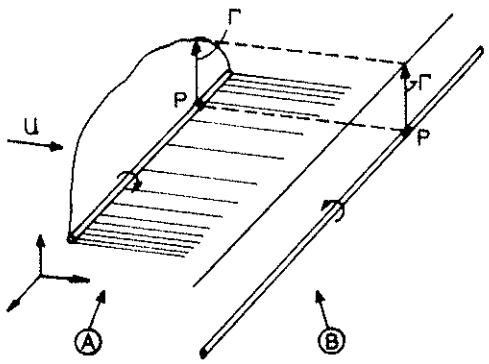

Fig.5: Definition of induced velocity in P: sum of contributions vortex systems Ⓐ and Ⓑ.

Things are very different however, when we come to consider unsteady flow (see fig. 6). Again, we should take for $v_i(z,t)$ the velocity due to the lifting vortex line (having a wake of trailing as well as shed vorticity) and add to this the velocity due to the two-dimensional vortex, which now also is accompanied by shed vorticity. It will be clear, that this definition of "induced velocity" does not lead to infinite values of $v_i(z,t)$. One of the deficiencies of the conventional lifting line approach to unsteady flow has thus been traced back to a wrong interpretation of Prandtl's steady flow model.

At the same time, the asymptotic approach to lifting line theory offers for the purpose of actual calculations a very efficient procedure to find v_i, as has been outlined in chapter 4.

Having obtained a rigorous definition of the induced velocity v_i for the unsteady case, we can write down the integral equation for the time dependent function $c_\ell(z,t)$. Let us assume that the rectangular wing considered is moving through a gust field, whose vertical velocity v_g in the XOZ-plane (fig. 4) is $v_g(x,z,t)$.

The pressure field of the wing has the same form as the pressure field (15), except that c_ℓ becomes a function of time:

$$\frac{p}{\frac{1}{2}\rho U^2} = -\frac{c_\ell(t;z)}{\pi}\frac{\sin\varphi}{\cosh\eta+\cos\varphi} +$$

$$+\frac{p_{dip}}{\frac{1}{2}\rho U^2}(r,\chi,z,t) + c_\ell(t;z)\, c\,\frac{\sin\chi}{2\pi r} \qquad (18)$$

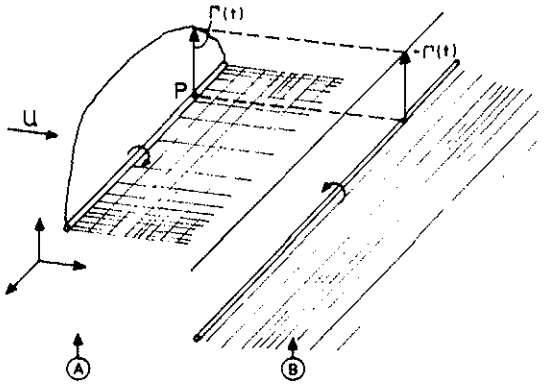

Fig.6: Definition induced velocity in unsteady flow.

It should be noted that this pressure field is entirely different from the field of a wing placed in a steady parallel flow, where the unsteadiness results from a pitching or heaving motion of the wing with respect to an inertial frame of reference. In the latter case the pitching motion of the wing surface implies a vertical acceleration of the particles of air moving along the wing surface, so that the near pressure field (18) would then have to be supplemented by an additional field taking care of this additional acceleration.

In expression (18) the near field is the pressure field of a two-dimensional flat plate aerofoil at rest with respect to an inertial frame of reference, although its lift is variable. The value of $v/U(z,t)$ along the mid-chord line contributed by the near pressure field should then be calculated according to the two-dimensional theory for an aerofoil in a gustfield, and is symbolically written like:

$$\left\{\frac{v}{U}(t;z)\right\}_{\text{near field}} = -\,f_{\text{2-d gust}}\{c_\ell(t;z)\} \qquad (19)$$

where the minus sign has been added just for convenience. Analogous to the development of steady lifting line theory, the final integral equation determining $c_\ell(t;z)$ may then be written in the form:

$$c_\ell(z,t) = f^{-1}_{\text{2-d gust}}\left\{\alpha_o(z) + \frac{v_g}{U}(0,z,t) - \frac{v_i}{U}(z,t)\right\} \qquad (20)$$

which states that a wing section behaves like a two-dimensional aerofoil which is at rest with respect to an inertial frame of reference and is placed in an "effective" gust field.

If α_o in (20) is a function of time $\alpha_o(z,t)$, then we have the case of a wing in pitching motion, and (20) does not remain valid. The wing sections may then be considered to behave like two-dimensional pitching aerofoils, whereas the induced downwash associated with the lift due to pitching may be considered as a "self-induced" gust field which adds to v_g. The unsteady lifting line theory thus takes the form:

$$c_\ell(z,t) = f^{-1}_{\text{2-d pitching}}\{\alpha_o(z,t)\} + f^{-1}_{\text{2-d gust}}\left\{\frac{v_g}{U}(0,z,t) - \frac{v_i}{U}(z,t)\right\} \qquad (21)$$

where v_i is caused by the <u>total</u> lift of the sections.

6. <u>The use of measured section characteristics</u>

As stated already in the introduction, one of the advantages of lifting line theory is that measured two-dimensional section characteristics may be substituted wherever the theory indicates two-dimensional relationships between c_ℓ and an effective angle of attack or an effective gust velocity. One of the questions then becoming relevant is: should one use in rotoranalysis the measured characteristics of an aerofoil in pitching motion, in heaving motion, or the characteristics of an aerofoil moving through a gust field?

If we consider eq. (13) expressing the pressure field of a helicopter blade, it is seen that the near pressure field not only consists of a "flat plate part" but also contains the field with F_1. The latter field is necessitated by the vertical acceleration to which the particles of air moving along the blade surface are subjected by the rather complicated motion of the blade. As shown in ref. 2, the pressure field with F_1 cannot be simulated in a wind tunnel by just giving the test aerofoil a pitching motion. To indicate the complexity of the case: the function $F_1(\psi_b, z_b)$ contains a component independent of ψ_b, which could only be simulated by giving the test aerofoil an "effective" camber. Fortunately, the field depending on F_1 is weak (A is in the denominator) whereas it has a low frequency content (0-, 1- and 2-P components only).

An obvious approximation would then be to treat all the non-steady effects of the blade section as <u>quasi-steady</u>, except of course the high intensity, high frequency variations of lift associated with the "flat plate" part of the pressure field, i.e. except the unsteadiness associated with the variations of the induced velocity v_i experienced by the blade sections. This implies, according to eq. (21), that the test aerofoil should be fixed with respect to the wind tunnel, whereas the tunnel flow should have a variable direction corresponding to the induced velocity variations.

This would still require a rather awkward experimental set-up, and it is hardly surprising that most actual experiments are carried out the other way round: the aerofoil oscillates in a steady parallel flow. However, one should be extremely cautious when interpreting the results so obtained!

The figures 7 through 10 show a comparison, based on theory, between a flat plate aerofoil in a gust field and a flat plate oscillating around its c/4-point. In both cases it is assumed that the angle between the chord and the free-stream velocity varies like:

$$\alpha(t) = \alpha_o \sin\omega t.$$

The lift coefficient $c_\ell(t)$ varies like

$$c_\ell(t) = c_{\ell_o} \sin(\omega t + \varphi)$$

where the amplitude c_{ℓ_o} would have the value $c_{\ell_o} = 2\pi\alpha_o$ in quasi-steady conditions. Fig. 7 shows the actual unsteady value of c_{ℓ_o} as a function of the reduced frequency $k = \frac{\omega c}{2U}$, and fig. 8 the phase angle φ.

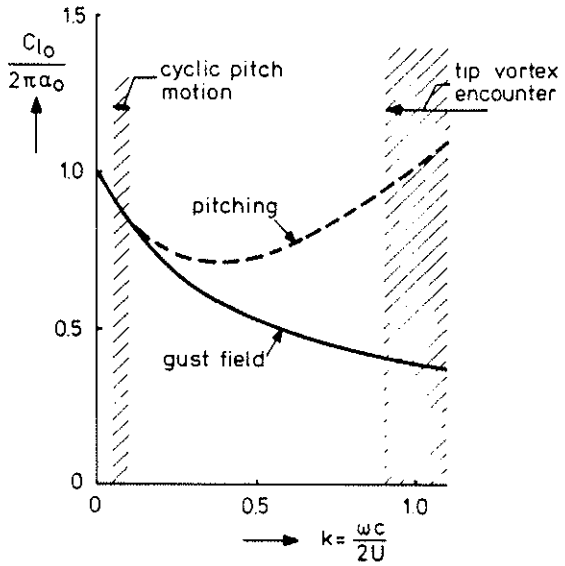

Fig. 7: Amplitude ratio vs reduced frequency of aerofoil in pitching motion and in oscillating flow.

It appears that for k of the order 0.1, which is a typical value for the relatively slow cyclic pitch motion, the two cases would not differ significantly. The wake induced angle of attack variations, however, are much faster than this. Actually, a blade section passing the tip vortex of a preceding blade may experience flow angle frequencies well above k = 1.0.

In this range of frequencies a wind tunnel experiment <u>not</u> simulating the real gust-like environment would make hardly any sense at all. This conclusion is enhanced by the figures 9 and 10, where the chordwise load distribution is shown as a function of time for the two cases. The reduced frequency is assumed to be large: k = 1.0. The differences shown illustrate clearly that the boundary layer development cannot but differ markedly between the two cases. One should thus be careful to simulate the flow conditions realistically when experimentally studying effects like dynamic stalling.

7. Lifting line theory in yawed flow

As a "model" case, we will again take a rectangular, uncambered wing whose mid-chord line includes a sweep angle Λ with the free-stream velocity U (notations: fig. 4). The pressure field of the wing is identical in form to that of the unswept wing:

$$\frac{p}{\frac{1}{2}\rho U^2} = -\frac{c_\ell(z)}{\pi}\frac{\sin\varphi}{\cosh\eta+\cos\varphi} + \frac{p_{dip}}{\frac{1}{2}\rho U^2}(r,\chi,z) +$$

$$+ c_\ell(z)\; c\,\frac{\sin\chi}{2\pi r} \qquad (22)$$

where the sectional lift coefficient is still defined as

$$c_\ell(z) = \frac{\ell(z)}{\frac{1}{2}\rho U^2 c} \qquad (23)$$

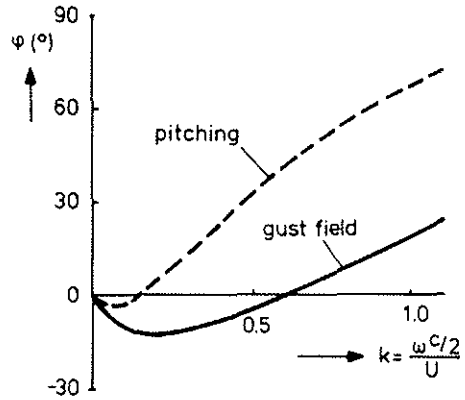

Fig. 8: Phase angle vs reduced frequency of aerofoil in pitching motion and in oscillating flow.

In order to calculate the vertical velocity perturbation at the mid-chord line, say at the section z_o, we consider a particle of air coming from far upstream and reaching the point $x = 0$, $z = z_o$ at time $t = 0$. At any instant t its position relative to the wing is known, and so is the value of $\partial p/\partial y(t)$ experienced by the particle. The value of v at the mid-chord line is then found by solving the integral

$$v(0,0,z_o) = -\frac{1}{\rho}\int_{-\infty}^{o}\frac{\partial p}{\partial y}(t)\,dt \qquad (24)$$

The induced velocity v_i is defined as v (with a minus sign) due to the pressure dipole line and the two-dimensional pressure dipole in eq. (22) and does not become singular in yawed flow since there occurs only a logarithmic singularity in the integrand of (24). The explanation of this marked difference with conventional lifting line theory is easy, when it is recognized that the case of yawed flow shows some resemblance with the earlier discussed case of unsteady flow. This is immediately clear when the lifting line itself with its trailing vorticity is considered (fig. 11). The skew trailing vortex sheet may be decomposed in a sheet with vorticity perpendicular to the lifting line, and a sheet with vorticity parallel to the lifting line. It is the latter vorticity which causes the singularities in conventional theory, just like the shed vorticity in the unsteady case. Now the asymptotic lifting line theory shows that there must also be taken into account a contribution to v_i due to the two-dimensional pressure dipole. The strength of the pressure dipole is (see eq. (22)) $\ell\{z(t)\}$. This is a variable dipole, since the z-coordinate of the considered particle varies

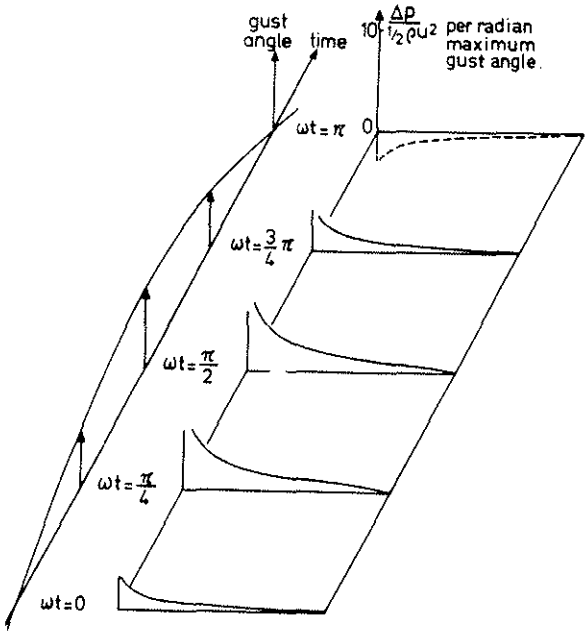

Fig. 9: Time history load distribution on an aerofoil moving through harmonic gust field, k = 1.0

as a function of time, due to its skewed trajectory with respect to the mid-chord line. Translated into vortex terminology, this means that from the velocity field depicted in fig. 11 a field must be subtracted which is associated with a variable two-dimensional vortex. The shed vorticity associated with the variable vortex suppresses the singular velocities. A rigorous definition of v_i in yawed flow can thus be given, analogous to the definition for unsteady flow depicted in fig. 6.

It is furthermore interesting to consider the velocity in the point z_o due to the near pressure field:

$$\frac{p}{\frac{1}{2}\rho U^2} = -\frac{c_\ell(z)}{\pi}\,\frac{\sin\varphi}{\cosh\eta+\cos\varphi} \qquad (25)$$

The value of $\partial p/\partial y$ due to the near field, experienced by the particle has the form

$$\frac{\partial p}{\partial y}(t) = \ell\{z(t)\}.\ f\{x(t)\} \qquad (26)$$

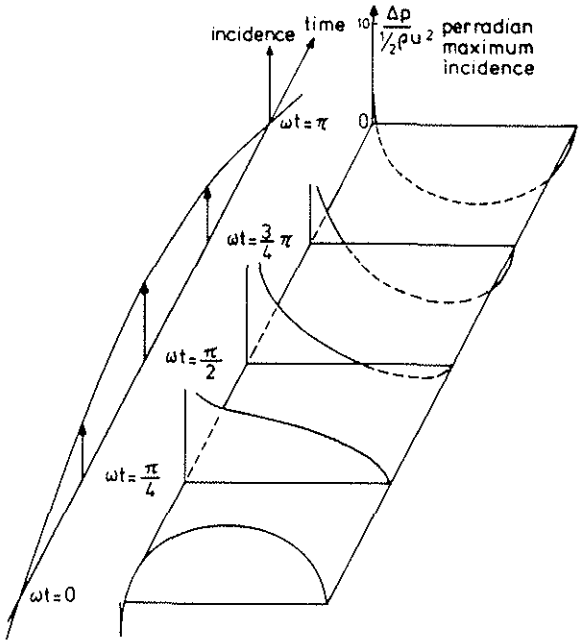

Fig 10: Time history load distribution on an aerofoil pitching around c/4 point, k=1.0

What the particle experiences, is equivalent to the acceleration due to the pressure field of a two-dimensional flat plate aerofoil, which it approaches with a relative velocity $\frac{dx}{dt} = U\cos\Lambda$. The lift of the equivalent aerofoil is variable in time, since z is a function of time. The analogy between the case of yawed flow and (nonperiodic) unsteady flow makes it possible to use unsteady aerofoil theory in order to find the contribution to v associated with the near pressure field. The derivation will not be given here, in view of its complexity caused by the non-periodic character of the equivalent unsteadiness. The final result for v/U found at the mid-chord line is:

$$\frac{v}{U\cos\Lambda}(z_o^*) = \frac{1}{\rho\pi c(U\cos\Lambda)^2}\left[-\ell(z_o^*)+\frac{\tan\Lambda}{A}\,\ell'(z_o^*)\,\ell n\left|\frac{\tan\Lambda}{2A}\right| + \right.$$

$$-\frac{\tan\Lambda}{A}\,\ell'(z_o^*)\,\ell n\left|\operatorname{sgn}\Lambda+z_o^*\right| +$$

$$\left.-\frac{\tan\Lambda}{A}\int_{-\operatorname{sgn}\Lambda}^{z_o^*}\frac{\ell'(\zeta^*)-\ell'(z_o^*)}{z_o^*-\zeta^*}\,d\zeta^*\right] +$$

$$-\frac{v_i}{U\cos\Lambda}(z_o^*) + O(A^{-2}) \qquad (27)$$

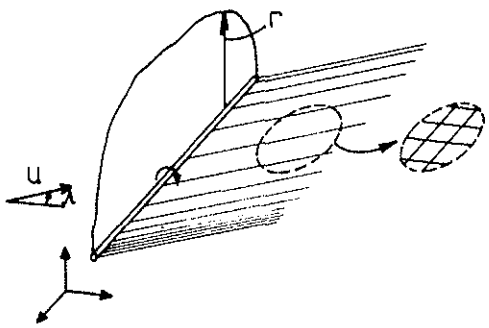

Fig.11: Trailing vorticity swept wing decomposed into vorticity perpendicular and parallel to lifting line.

where z^* and ζ^* denote spanwise coordinates non-dimensionalized by b/2, ℓ' denotes the derivative w.r. to z^*, and $\operatorname{sgn}(\Lambda) = \pm 1$ according to the sign of the sweep angle Λ.

If the incidence of the wing with respect to the XOZ-plane is denoted as α_o, the vertical velocity at the mid-

chord line should become $v(z^*_o) = -\alpha_o U\cos\Lambda$ which on substitution into (27) completes the integral equation for $\ell(z^*_o)$. Let us neglect for a moment the terms in eq. (27) involving $\tan\Lambda/A$. The integral equation then becomes:

$$\ell(z) = 2\pi(\alpha_o - \frac{v_i}{U\cos\Lambda}) \tfrac{1}{2} \rho(U\cos\Lambda)^2 c \qquad (28)$$

This is the familiar result stating that the wingsections behave as two-dimensional aerofoils at an effective angle of attack in a flow with free-stream velocity $U\cos\Lambda$. It should be noted that this result is obtained by neglecting terms of order $0(\tan\Lambda/A)$ in eq. (27). Since lifting line theory itself neglects only terms of $0(A^{-2})$ the simplification leading to the simple $\cos\Lambda$-sweep correction is not consistent with lifting line theory, unless Λ is very small.

In order to give an impression of the errors which may be introduced by using the simple $\cos\Lambda$ sweep correction, fig. 12 has been prepared. A rectangular wing in parallel flow is considered whose twist distribution is assumed to be such that, using the simple $\cos\Lambda$ correction, a lift distribution results as given by the solid line in fig. 12. This is an asymmetrical distribution typical for rotating blades, although in the case of helicopter blades the asymmetry would not be caused by twist, but would instead result from the "free-stream" velocity increasing towards the tip. Using the c_ℓ-distribution drawn in fig. 12 as a starting point, the terms of eq. (27) depending upon $\tan\Lambda/A$ have been evaluated and have been used to determine a new liftdistribution as shown by the dotted lines in fig. 12. Iterating further would theoretically add non-relevant further corrections of order A^{-2}. However, it may be seen that the dotted distributions lead to errors in the wing tip regions, since c_ℓ no longer vanishes at the tips. In practice therefore, eq. (27) would be solved by considering it as an integral equation, which procedure prevents such problems. Nevertheless, fig. 12 shows very well the primary effects of the additional sweep correction terms of eq. (27), being a "phase shift" and an amplitude decrease of the lift.

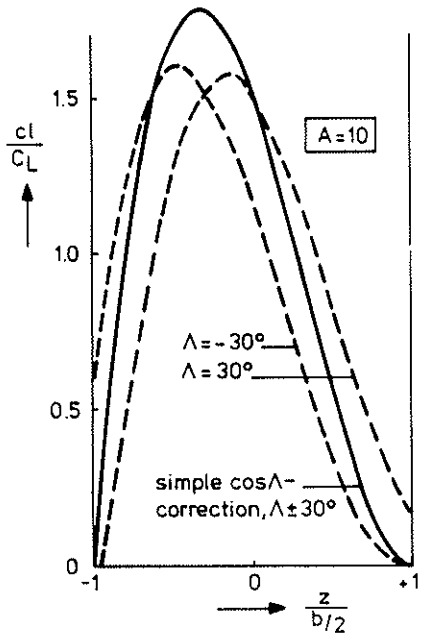

Fig.12: Error due to simple sweep correction.

3. The assumption of approximate two-dimensionality of the sections

In chapter 4 it was shown that the assumption of approximate two-dimensionality of the blade sections is valid up to order $0(A^{-1})$. In the next higher order approximation, taking into account terms of $0(A^{-2})$, the near field satisfies the two-dimensional Poisson equation (12). The far field in a higher-order theory also becomes more complex: it is given by a line of pressure dipoles as well as quadrupoles. If we again consider the model case of a rectangular wing in parallel flow, it may be shown (refs. 2 and 3) that the liftdistribution finally becomes:

$$\ell(z^*) = 2\pi\tfrac{1}{2}\rho U^2\{\alpha_o(z^*) - \frac{v_i}{U}(z^*)\} + \frac{\ell''(z^*)}{2A^2}\{\tfrac{1}{2} + \ln 4A + \tfrac{1}{2}\ln(1-z^{*2})\} +$$

$$+ \frac{1}{4A^2}\int_{-1}^{+1} \frac{\ell''(\zeta^*) - \ell''(z^*)}{|\zeta^* - z^*|}\, d\zeta^* \qquad (29)$$

where z^* and ζ^* again denote spanwise coordinates non-dimensionalized by b/2, and ℓ'' is the second spanwise derivative of lift w.r. to z^*.
It appears that classical lifting line theory will be unsatisfactory if the second spanwise derivative of the lift attains large values. This is often so in the case of helicopterblades.

In order to give an impression of the order of magnitude of the higher order terms, fig. 13 has been prepared. The full line in this figure is assumed to be the liftdistribution as determined by classical lifting line theory. The dotted line is the liftdistribution as found by adding the higher order terms. The classical lifting line theory may clearly lead to significant errors for the type of liftdistribution existing on helicopterblades. The non-vanishing of the lift at the wing tips may again be prevented by treating eq. (29) as an integral equation (see ref. 2).

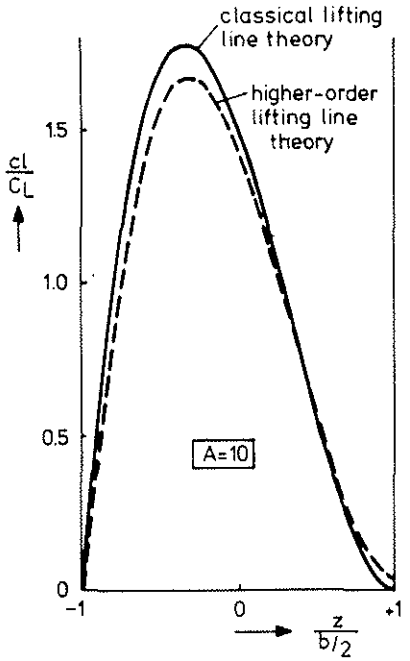

Fig.13: Error due to assumption of sectional two-dimensionality.

It may be shown that the resulting integral equation is, in the case of a rectangular wing in steady parallel flow, equivalent to Weissinger's 3/4-chord point method. Fig. 14 shows a comparison, taken from ref. 4, of results for a flat plate rectangular wing obtained by classical lifting line theory, higher order lifting line theory, and a lifting surface theory. It appears that the discrepancy between the classical lifting line theory and lifting surface theory can be removed almost entirely by adding the terms of order $0(A^{-2})$ as is done in the higher order lifting line theory. The higher order theory derived by an asymptotic method has several advantages compared with Weissinger's method:
a) it remains valid in unsteady flow, whilst the 3/4-chord method does not,
b) it gives information about the changes in pressure distribution over the wing-chords due to the higher order effects.

In order to illustrate the latter point, fig. 15 shows the position of the local centres of pressure for the dotted lift distribution of fig. 13, as calculated by the higher order asymptotic theory. The figure indicates a significant shift of the centres of pressure as compared with conventional lifting line theory.

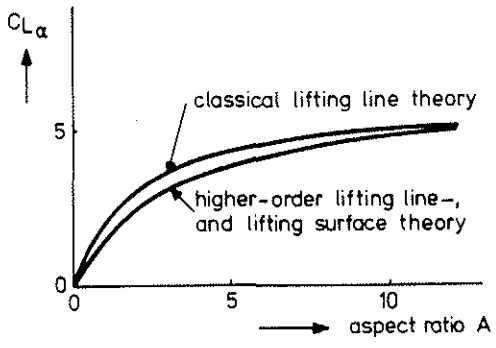

Fig. 14: Accuracy of lifting line theories.

9. Conclusions

Using as a simple model a rectangular wing in parallel flow having a spanwise liftdistribution typical for helicopterblades, the validity of conventional lifting line analysis and related concepts has been examined. This was done by first deriving more complete expressions by an asymptotic theory, and then showing the form and order of magnitude of the terms neglected in conventional lifting line theory. It is concluded that:
a) The singular behaviour of the in-

duced velocity in unsteady and yawed flow associated with a continuous trailing vortex sheet is due to a misinterpretation of Prandtl's original steady flow theory. A satisfactory definition of v_i can be derived.
b) The simple cosΛ-sweep correction is inconsistent with lifting line theory and may lead to very large errors.
c) The use of measured section characteristics in a lifting line analysis requires experiments on a fixed aerofoil placed in an oscillating flow. Wind tunnel results obtained from oscillating aerofoils may be erroneous in the range of high values of the reduced frequency, especially when it is tried to extract the dynamic stall behaviour.
d) The assumption of approximate two-dimensional behaviour of blade sections may lead to significant errors when the second spanwise derivative ℓ'' of the lift is relatively large. Especially the position of the sectional centres of pressure may be affected by large values of ℓ''.

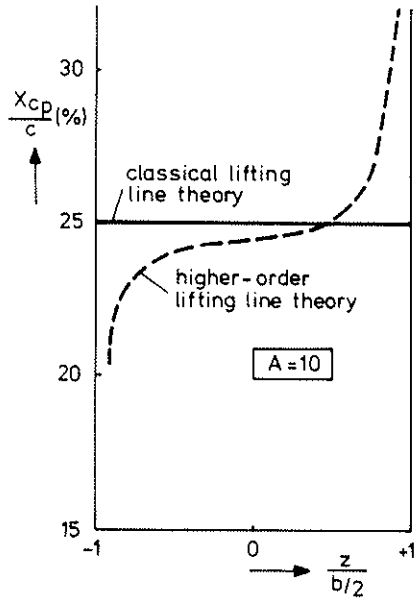

Fig.15: Position of sectional centres of pressure. Lift distribution of fig.13.

Remedies for the above mentioned problems have been derived: an asymptotic theory suitable for helicopter rotor calculations has been described in refs. 2 and 3 which correctly takes into account all the unsteady, yawed flow effects of inviscid theory, to an order of accuracy comparable with lifting surface theory, with computational efforts comparable with conventional lifting line theory.
It is also conceivable to use the expressions given in the present paper, valid for the rectangular wing, as approximate corrections to be incorporated into conventional lifting line theory. This approach - approximate, but perhaps more convenient and efficient than the exact procedure of ref. 2 - to helicopter blade analysis is at present being investigated by the author.

10. References

1. B.M. Rao, W.P. Jones: Application to rotary wings of a simplified aerodynamic lifting surface theory for unsteady compressible flow. Paper presented at the AHS/NASA-Ames specialists' meeting on rotorcraft dynamics, Feb. 1974.
2. Th. van Holten: The computation of aerodynamic loads on helicopter blades in forward flight, using the method of the acceleration potential, Dissertation Delft University of Technology, March 1975.
   Also published as Report VTH-189, March 1975.
3. Th. van Holten: Computation of aerodynamic loads on helicopter rotorblades in forward flight, using the method of the acceleration potential, ICAS-paper No. 74-54 presented at the 9th Congress of the International Council of the Aeronautical Sciences, Haifa 1974.
   Also to be published in the Proceedings of the 9th ICAS Congress, Haifa 1974.
4. H. Schlichting, R. Truckenbrot: Aerodynamik des Flugzeuges, Springer-Verlag 1969.